ELSEVIER

Journal of Biomechanics 38 (2005) 87–97

JOURNAL OF BIOMECHANICS

www.elsevier.com/locate/jbiomech
www.JBiomech.com

Mechanics of the taper integrated screwed-in (TIS) abutments used in dental implants

Dinçer Bozkaya, Sinan Müftü*

Department of Mechanical Engineering, Northeastern University, 334 Snell engineering, Boston, MA 02115, USA

Accepted 17 March 2004

Abstract

The tapered implant–abutment interface is becoming more popular due to the mechanical reliability of retention it provides. Consequently, understanding the mechanical properties of the tapered interface with or without a screw at the bottom has been the subject of a considerable amount of studies involving experiments and finite element (FE) analysis. This paper focuses on the tapered implant–abutment interface with a screw integrated at the bottom of the abutment. The tightening and loosening torques are the main factors in determining the reliability and the stability of the attachment. Analytical formulas are developed to predict tightening and loosening torque values by combining the equations related to the tapered interface with screw mechanics equations. This enables the identification of the effects of the parameters such as friction, geometric properties of the screw, the taper angle, and the elastic properties of the materials on the mechanics of the system. In particular, a relation between the tightening torque and the screw pretension is identified. It was shown that the loosening torque is smaller than the tightening torque for typical values of the parameters. Most of the tightening load is carried by the tapered section of the abutment, and in certain combinations of the parameters the pretension in the screw may become zero. The calculations performed to determine the loosening torque as a percentage of tightening torque resulted in the range 85–137%, depending on the values of taper angle and the friction coefficient.
© 2004 Elsevier Ltd. All rights reserved.

Keywords: Dental implants; Taper lock; Morse taper; Conical interference fit; Tapered screw; Screw mechanics; Loosening torque; Tightening torque

1. Introduction

A dental implant system serves as the anchor for the prosthetic reconstruction of missing teeth by supporting a fixed or removable prosthesis. The system mainly consists of an implant and an abutment. *A prosthetic attachment* is typically fixed on the *abutment* by one of the following methods: cementation, use of an occlusal screw, or a socket arrangement that allows retention of a removable prosthesis. The *implant* is the component implanted into the jaw bone, and the *abutment* is the component which supports and/or retains the prosthesis (Misch, 1999). The abutment is secured to the implant with a mechanical attachment method, and ideally it should stay fixed with respect to the implant throughout the life of the implant. In the most common mechanical attachment method, a retaining-screw (abutment screw) is used to fix the abutment with respect to the implant (Misch, 1999). Another approach is to use a screw with a relatively large tapered end. In this paper, the term *taper integrated screwed-in* (TIS) abutment is used to indicate an abutment which uses simultaneously a screw and a tapered fit. A tapered interference fit (TIF) between the abutment and the implant is also used in some implant systems to provide the connection. The mechanics of the attachment method using the retaining-screw can be analyzed based on classical power screw formulas (Shigley and Mischke, 1989) and the finite element method (Lang et al., 2003). The mechanics of the TIF-type attachment method has been investigated with approximate closed-form formulas by the authors (Bozkaya and Müftü, 2003). The subject of this paper is the mechanical analysis of the TIS-type attachment method, which has been previously investigated using the finite element method (Merz et al., 2000).

*Corresponding author. Tel.: +1-617-373-4743; fax: +1-617-373-2921.
E-mail address: smuftu@coe.neu.edu (S. Müftü).

0021-9290/$ - see front matter © 2004 Elsevier Ltd. All rights reserved.
doi:10.1016/j.jbiomech.2004.03.006

Four commercially available implant systems are shown in Fig. 1. The design by Nobel Biocare (Nobel Biocare AB, Göteborg, Sweden) uses a retention-screw, the designs by Ankylos (Degussa Dental, Hanau-Wolfgang, Germany) and ITI (Institut Straumann AG, Waldenburg, Switzerland) use TIS-type abutments; and the design by Bicon (Bicon Inc., Boston, MA, USA) uses the TIF-type abutment. A 2001 market survey in the United States indicates that nearly 85% of the implant sales involve implant systems using retaining-screws and 15% involve a system using the TIS-type abutments (Anonymous, 2001). The TIF-type abutments are not included in this survey, but they have a small market share.

In general, the reliability and the stability of an implant–abutment connection mechanism is an essential prerequisite for long-term success of dental implants (Scacchi et al., 2000). Screw complications, such as loosening, had been encountered with the screw-type implant–abutment connection mechanism, in particular in single tooth replacement scenarios (Geng et al., 2001; Schwarz, 2000). Inadequate preload, the misfit of the mating components and rotational characteristics of the screws were considered to be the reasons leading to screw loosening or fracture (Schwarz, 2000). Design improvements and using gold, as screw material, resulted in significant improvements (Misch, 1999) in the loosening incidences encountered early on, in systems using titanium retention screws (Jemt et al., 1991; Becker and Becker, 1995). Application of a sufficiently high tightening torque has also been shown to have a positive effect in preventing retention-screw loosening incidences, in a 5-year follow-up study (Haas et al., 1995,2002). Various longitudinal follow-up studies involving the abutment screw CeraOne (Nobel Biocare AB, Göteborg, Sweden) show that the screw complications have been avoided with this design in single tooth restorations (Andersson et al., 1995; Bianco et al., 2000; Scheller et al., 1998; Wannfors and Smedberg, 1999). The attachment mechanism using a retention screw is now widely used by the clinicians (Anonymous, 2001), perhaps in great part based on the reliability of the screw retention system.

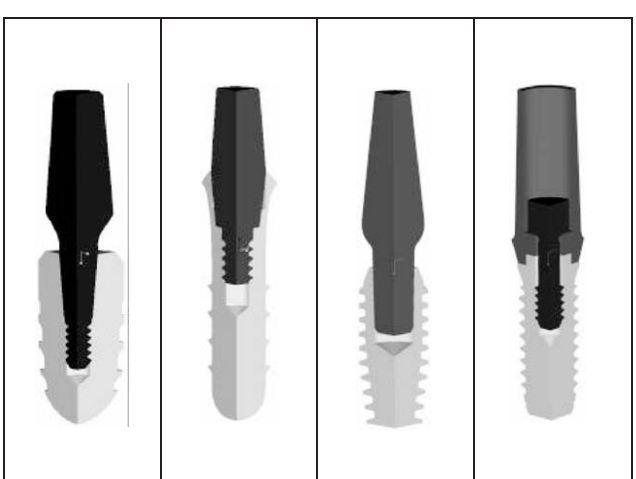

Fig. 1. Various implant–abutment attachment methods.

The TIS-type abutment offers a high resistance to loosening torques in single tooth replacements, as it will be shown in this paper. A multicenter retrospective study of 174 single implants investigated the success rate of the ITI implant system, for 6 month (Levine et al., 1997) and 2 year (Levine et al., 1999) periods. Abutment loosening occurred in 3.6% and 5.3% of the implants in these periods, respectively. In another 5-year follow-up study involving 114 ITI solid screw implants, only one abutment loosening incidence was reported (Behneke et al., 2000). In a 6-month follow-up study of Ankylos system (Aryatawong and Kamolpan, 1998), abutment loosening has not been encountered in any of the 74 implants, even in the posterior region where the implants are subjected to high occlusal loads. It has also been reported that loosening of the abutment is prevented if the recommended tightening torque value of 250 N mm is applied to straight Ankylos abutments (Romanos and Nentwig, 2000). Although the studies show high success rates of TIS implants with respect to abutment loosening, longer term studies are needed to evaluate the implant–abutment stability since fatigue loading may be the mode of failure. Difficulty of retrievability could be considered as a disadvantage of the TIS-type abutments (Squier et al., 2002). Clinical studies showing the success of the TIS-type implant–abutment interface encouraged the researchers and implant companies to focus on understanding and evaluating the mechanical properties of the tapered interface.

An experimental study by Norton (Norton, 1999) investigated the variation of the loosening torque as a percentage of tightening torque with respect to different parameters such as tightening torque (40–500 N mm), taper angle (8° and 11°), interfacial surface area (15.3 and 27.9 mm^2), existence of saliva contamination and time delay to loosening (10 and 60 min). Strong correlation was found between loosening torque as the percentage of tightening torque. The taper angle, saliva contamination and time delay to loosening did not have a significant effect on the loosening torque, whereas the interfacial surface area seemed to have a profound effect on the efficiency of the connection. The *efficiency* is defined as the ratio of the loosening torque to the tightening torque. At clinically relevant torque levels (300–400 N mm), the loosening torque was 84–91% of the tightening torque. This finding was in contrast to the experimental work done by Sutter et al. (1993), who showed the loosening torque to be 10–15% higher than the tightening torque. It was also shown that dynamic

loading resulted in 50% reduction of the loosening torque; however, no decrease occurred in cone-screw connection after 1 million cycles (Sutter et al., 1993). The 8° taper angle with 2 mm diameter screw at the bottom was selected to be the optimum design that provides a secure assembly between implant and abutment. Squier et al. (2002) investigated the effects of anodization and reduction of surface area on the tightening and loosening torque. A 31% reduction of surface area did not cause a significant change in the loosening torque, however the surface coating caused a 20% decrease in the loosening torque. In their study, for 350 N mm tightening torque, the loosening torque was in the range of 79–106% of the tightening torque.

The strength of the tapered interface in a TIS abutment was assessed by experimental and finite element methods. The tapered interface was found to be favorable in terms of resistance to bending forces (Norton, 2000). The stresses induced by off-axis loads were compared for tapered and butt-joint connection. It was concluded that the tapered interface distributed the stresses more evenly when compared to the butt joint connection (Merz et al., 2000). The conical interface allowed a larger maximum tightening torque. The maximum tightening torque was 4000 N mm for the TIS abutment, which was considerably greater than the 1250 N mm of the screw-only connection (Sutter et al., 1993).

Bacterial leakage through implant–abutment interface is another significant factor affecting the long-term stability of the implant (Jansen and Richter, 1997). Although the tapered interface is considered to be acting as a seal against bacterial leakage and colonization, it cannot completely prevent leakage due to the gap caused by the misfit between the components. The rate of bacterial leakage diminishes as the degree of misfit decreases and the tightening torque of the screw increases (Jansen and Richter, 1997).

The mechanics of the purely TIF-type implants was first explained by O'Callaghan et al. (2002) and then by Bozkaya and Müftü (2003,2004). Approximate analytical solutions for the contact pressure, the pull-out force and loosening torque acting in a tapered interference were developed by modeling the tapered interference as a series of cylindrical interferences with variable radii. These formulas compared favorably with non-linear finite element analyses for different design parameters (Bozkaya and Müftü, 2003).

In this paper, approximate closed-form formulas are developed for estimating the tightening and loosening torque magnitudes for the TIS-type abutment connections. The closed form equations for the tapered interference fit (Bozkaya and Müftü, 2003) are combined with screw mechanics equations to determine the loosening and tightening torque as a function of various design parameters. The *efficiency* of the system, defined as the ratio of the loosening torque to the tightening torque, is investigated.

2. Theory

A taper integrated screwed-in (TIS) abutment is placed into the implant by applying a tightening torque T_T. The tightening process causes interference in the tapered part and also advances the screw, which in turn causes the threads of the abutment and the implant to engage with a positive force. This results in a tensile load in the screw known as the *preload*.

The geometric parameters that affect the mechanics of the connection are defined in Fig. 2 where the implant is depicted as a cylinder. The balance of forces and torques acting on this system during tightening are evaluated using the free body diagrams given in Figs. 3 and 4. During tightening, the screw preload F_T^r will be related

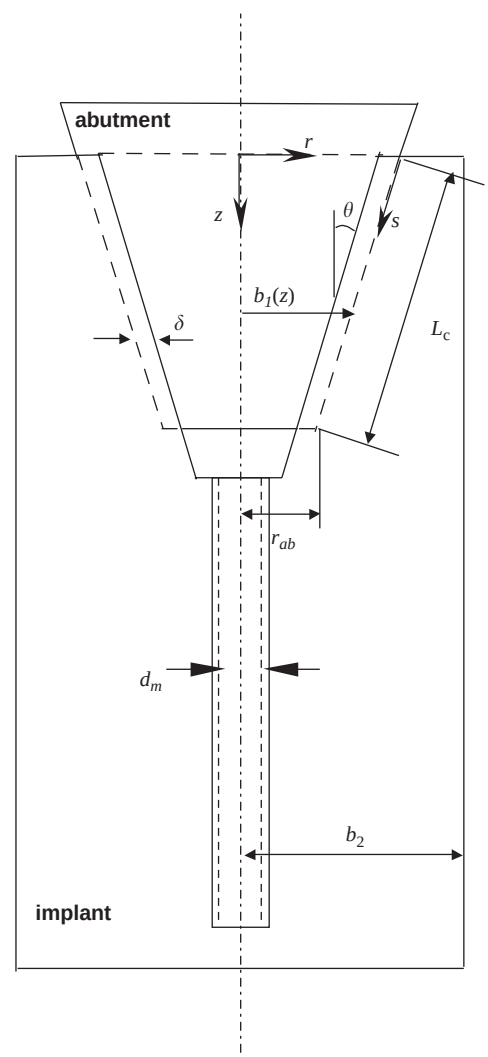

Fig. 2. The geometric parameters that affect the mechanics of the TIS-type abutment–implant attachment method.

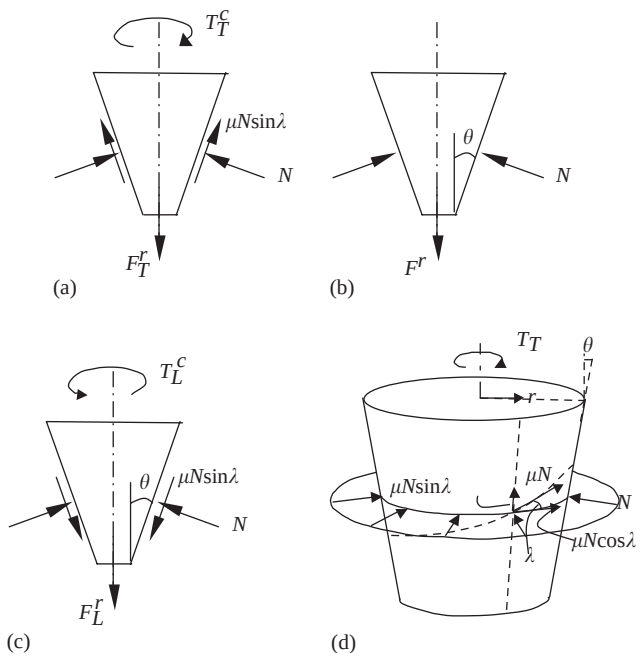

Fig. 3. The FBD diagrams of the tapered section of the TIS-type abutment during (a) tightening, (b) functional loading, and (c) loosening, give the corresponding pre-tension levels F_T^r, F^r and F_L^r caused in the screw as shown in this figure. (d) Friction force in tightening.

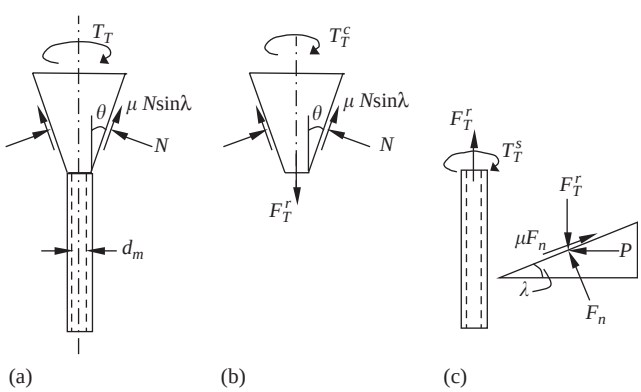

Fig. 4. (a) Free body diagram (FBD) of the taper integrated screwed-in (TIS) abutment during tightening. (b) The FBD of the tapered section of the TIS abutment. (c) The FBD of the screw section of the TIS abutment. Note that the total tightening torque T_T is equal to the torque required to tighten the tapered section T_T^c and the screw section T_T^s.

to the resultant normal force N, acting on the tapered section due to the interference fit. Thus by using, the well-known, power screw relations (Shigley and Mischke, 1989) and the tapered interference fit equations given by Bozkaya and Müftü (2003) it is possible to develop closed-form relations for the tightening and loosening of TIS-type abutments.

The resultant normal force N due to interference fit in the tapered section of the abutment, shown in Fig. 3a, is given as (Bozkaya and Müftü, 2003),

$$N = \frac{\pi E \Delta z\, L_c \sin 2\theta}{6b_2^2}\left[3(b_2^2 - r_{ab}^2) - L_c \sin\theta(3r_{ab} + L_c \sin\theta)\right], \quad (1)$$

where L_c is the contact length, b_2 is the outer radius of the implant, r_{ab} is the bottom radius of the abutment, θ is the taper angle as shown in Fig. 2, Δz is the axial displacement of the abutment during tightening, and, E is the elastic modulus of implant and abutment, assumed to be made of the same material.

2.1. The screw preload

When a TIS-type abutment is screwed into the implant, a tensile *preload*, develops in the screw and a *resisting force* F_T^r along the main axis of the abutment develops in the tapered part. This resisting force and the screw preload are equal in magnitude. The resisting force F_T^r has contributions due to friction force μN and the normal force N, and it can be found from the free body diagram in Fig. 3a. Note that the friction force develops along a helical path, as shown Fig. 3d, whose helix angle is equal to the lead angle $\lambda(=a \tan l/\pi d_m)$ of the screw.

Once the tightening torque is released, the frictional component of the preload diminishes, and the screw preload during functional loading, F^r, is determined from the free body diagram given in Fig. 3b. During loosening, the friction force acts in the opposite direction as compared to the tightening. The screw preload during loosening can be determined from Fig. 3c.

2.2. Tightening torque

The *total tightening torque* T_T required to screw-in the TIS abutment should overcome the resistive torque values T_T^s and T_T^c due to friction in the screw threads and the conical (tapered) interface, respectively (Fig. 4),

$$T_T = T_T^s + T_T^c. \quad (2)$$

The resistive torque T_T^s in the screw threads can be calculated by the power screw formula (Shigley and Mischke, 1989) for raising a load F_T^r,

$$T_T^s = \frac{F_T^r d_m}{2}\left(\frac{l + \pi\mu_k d_m \sec\alpha}{\pi d_m - \mu_k l \sec\alpha}\right), \quad (3)$$

where d_m is the mean diameter of the screw, μ_k is the kinetic friction coefficient, α is the thread angle and l is the lead of the screw. Note that the vertical resisting load F_T^r is used in this equation, as it is equal to the screw preload as mentioned above. The vertical component of the resisting force F_T^r in the tapered section,

during tightening is determined from Fig. 4a as

$$F_T^r = N\sin\theta + \mu_k N\sin\lambda\cos\theta, \tag{4}$$

where the kinetic friction coefficient μ_k is used, as screw tightening is a dynamic process.

In order to find an expression for the resistive torque T_T^c in the conical section of the abutment, the friction forces on the tapered section are considered. The horizontal component of the friction force, μN cos λ, in the conical interface, shown in Fig. 3d, resists the tightening torque. The torque required to overcome this friction force is found as follows (Bozkaya and Müftü, 2003):

$$\begin{aligned} T_T^c &= \left(2\pi\mu_k\int_0^{L_c\cos\theta} b_1^2(z)P_c(z)\,dz\right)\cos\lambda \\ &= \frac{\pi\mu_k E\Delta z L_c\sin 2\theta\cos\lambda}{8b_2^2}\{L_c\sin\theta[2(b_2^2-3r_{ab}^2) \\ &\quad - L_c\sin\theta(4r_{ab}+L_c\sin\theta)] + 4r_{ab}(b_2^2-r_{ab}^2)\}, \end{aligned} \tag{5}$$

where P_c is the contact pressure whose magnitude varies in the z-direction as described by Bozkaya and Müftü (2003). An equation for the total tightening torque T_T is obtained by combining Eqs. (1)–(5)

$$\begin{aligned} T_T &= \frac{d_m F_T^r}{2}\left(\frac{\pi\mu_k d_m\sec\alpha + l}{\pi d_m - \mu_k l\sec\alpha}\right) \\ &\quad + \frac{\pi\mu_k E\Delta z L_c\sin 2\theta\cos\lambda}{8b_2^2}\{L_c\sin\theta[2(b_2^2-3r_{ab}^2) \\ &\quad - L_c\sin\theta(4r_{ab}+L_c\sin\theta)] + 4r_{ab}(b_2^2-r_{ab}^2)\}, \end{aligned} \tag{6}$$

where the axial component of resistive force (preload) during tightening F_T^r is given by Eq. (4).

2.3. Loosening torque

An expression for the *total loosening torque* T_L, which equals the sum of the resistive torque values in the screw threads T_L^s and in the cone T_L^c due to friction, can be found by a similar approach. The total loosening torque is

$$T_L = T_L^s + T_L^c. \tag{7}$$

The resistive torque T_L^s in the screw threads is calculated from the power screw formulas. The free body diagram given in Fig. 3c shows that the preload at the onset of loosening F_L^r is expressed as

$$F_L^r = N\sin\theta - \mu_s N\sin\lambda\cos\theta, \tag{8}$$

where the static friction coefficient μ_s is used at the onset of loosening. Note that during loosening, the friction force acts in opposite direction as compared to the tightening case Fig. 3d. This results in the negative sign for the frictional component in this equation.

Inspection of Eq. (8) shows that the vertical resisting force F_L^r in the cone during loosening could take a positive or negative value, depending on the magnitude of the friction coefficient μ_s, taper angle θ and screw lead angle λ. Positive value of F_L^r implies that the resultant force in the conical interference is in the direction of the screw motion and negative value of F_L^r implies that the screw threads have lost contact. Hence, the torque formula required to lower a load should be used when $F_L^r > 0$, and no torque is transferred to the screw threads when $F_L^r > 0$. Torque T_L^s in the screw threads due to the preload is found from the power screw formula for lowering a load (Shigley and Mischke, 1989),

$$T_L^s = \frac{F_L^r d_m}{2}\left(\frac{\pi\mu_s d_m\sec\alpha - l}{\pi d_m + \mu_s l\sec\alpha}\right)H(F_L^r), \tag{9}$$

where H is the Heaviside step function defined as $H(F_L^r) = 1$ when $F_L^r > 0$ and $H(F_L^r) = 0$ when $F_L^r < 0$.

The resistive torque in the cone T_L^c is obtained by using the same procedure as in the case of tightening torque given in Eq. (5), by using the static friction coefficient μ_s instead of the dynamic friction coefficient μ_k,

$$\begin{aligned} T_L^c &= \frac{\pi\mu_s E\,\Delta z L_c\sin 2\theta\cos\lambda}{8b_2^2}\{L_c\sin\theta[2(b_2^2-3r_{ab}^2) \\ &\quad - L_c\sin\theta(4r_{ab}+L_c\sin\theta)] + 4r_{ab}(b_2^2-r_{ab}^2)\}. \end{aligned} \tag{10}$$

The total loosening torque T_L is obtained from Eqs. (7)–(10) as follows,

$$\begin{aligned} T_L &= \frac{d_m F_L^r}{2}\left(\frac{\pi\mu_s d_m\sec\alpha - l}{\pi d_m + \mu_s l\sec\alpha}\right)H(F_L^r) \\ &\quad + \frac{\pi\mu_s E\Delta z L_c\sin 2\theta\cos\lambda}{8b_2^2}\{L_c\sin\theta[2(b_2^2-3r_{ab}^2) \\ &\quad - L_c\sin\theta(4r_{ab}+L_c\sin\theta)] + 4r_{ab}(b_2^2-r_{ab}^2)\}, \end{aligned} \tag{11}$$

where the axial component of resistive force during loosening F_L^r is given by Eq. (8). The efficiency of TIS connection is defined as the ratio of the loosening torque to the tightening torque,

$$\eta_s = \frac{T_L}{T_T}. \tag{12}$$

3. Results

The formulas developed above are implemented to two implant systems, whose parameters are similar to a 4.8 mm diameter ITI system and a 5.5 mm diameter Ankylos system, as given in Table 1. Fig. 5 shows the effect of tightening torque T_T and friction coefficient μ_k on the radial interference, $\Delta u = \Delta z\tan\theta$, in the tapered section of the implant. In clinical practice, the abutment is secured into the implant by using the recommended torque value; therefore, T_T is the controlled variable. This figure shows that depending on the friction coefficient, the recommended torque value will be achieved with a different amount of radial interference. Radial interference values of $\Delta u = 5\,\mu$m and $0.75\,\mu$m

Table 1
Design parameters for an ITI-like and an Ankylos-like system

	Base values		Range of parameters
	ITI	Ankylos	Both systems
Taper parameters			
θ (°)	8	5.5	1–10
μ	0.3	0.3	0.1–1
μ_k/μ_s	1	1	0.7, 0.9, 1
L_c (mm)	0.731	3	0–5
b_2 (mm)	2.24	2.76	1–4
Δz (μm)	5	0.75	0–5
r_{ab} (mm)	1.42	0.97	—
E (GPa)	113.8	113.8	—
d_m (mm)	0.875	1.49	—
l (mm)	0.44	0.35	—
λ (°)	9.11	4.3	—
α (°)	30	27.5	—

The parameters were taken from an ITI implant: 043.241S and the matching ITI-abutment: 048.542; and from the Ankylos part number 3101-0053.

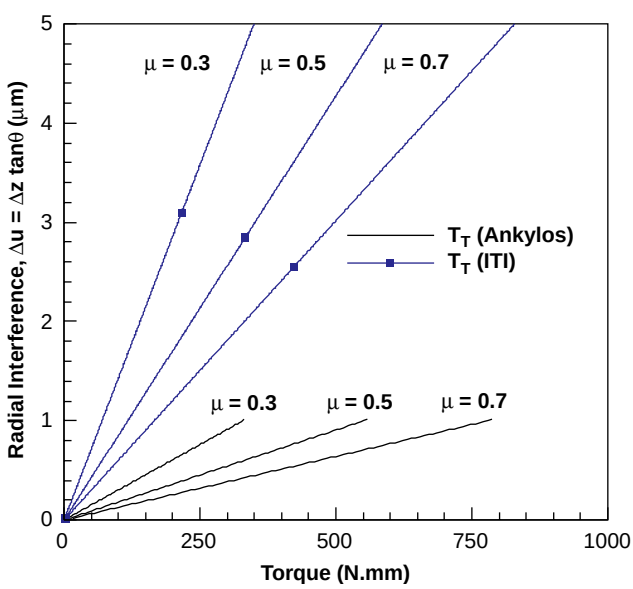

Fig. 5. Variation of the radial interference $\Delta u = \Delta z \tan\theta$ as a function of tightening torque T_T and friction coefficient $\mu_s = \mu_k = \mu$ for both ITI-like and Ankylos-like systems. Other parameters are given in Table 1.

were found, for $\mu_k = \mu_s = 0.3$, from this figure, for the ITI- and Ankylos-like systems, whose recommended torque values are 350 N mm (Norton, 2000) and 250 N mm (Anonymous, 2003), respectively. These values have been used in this paper.

3.1. The efficiency of the attachment

The efficiency η_s defined by Eq. (12) is plotted as a function of the static μ_s and kinetic μ_k friction coefficients and the taper angle θ in Fig. 6 for the Ankylos- and ITI-like geometries. The effect of friction is presented in Figs. 6a and b. These figures show that the efficiency of the system has a stronger dependence on the kinetic friction coefficient than the static friction coefficient. For example, when static and kinetic friction coefficients are equal, and vary in the 0.1–1 range, the efficiency varies between 0.87–0.92 for ITI and 0.84–0.94 for Ankylos; however, when kinetic friction coefficient is 70% of the static friction coefficient, the efficiency varies between 1.22–1.32 for ITI and 1.28–1.34 for Ankylos. According to Eq. (6) the kinetic friction coefficient only affects the tightening torque. Therefore, high efficiency is obtained if the kinetic friction coefficient during tightening is smaller than the static friction coefficient. Maximum efficiency is obtained when μ is between 0.3 and 0.4. Fig. 6a also shows the results of the experimentally obtained efficiency η_s values by Norton (1999) (0.86–0.91), Squier et al. (2002) (0.85–1.06) and Sutter et al. (1993) (1.1–1.5). The comparison shows that the results predicted by Eq. (12) and the experiments agree favorably.

Figs. 6c and d show the effect of using different taper angles (θ) for the Ankylos- and ITI-like geometries, respectively. In general, this figure shows that the efficiency of the system is reduced at larger taper angles. For example, for the case where $\mu_s = \mu_k = 0.5$ the efficiency drops from 0.96 to 0.915 for ITI and from 0.945 to 0.925 for Ankylos, as the taper angle increases from 1° to 10°. The slope change observed near θ=4.6° for ITI and near θ =2.2° for Ankylos, corresponds to the case where the screw preload F_L^r becomes zero, as predicted by Eq. (8). When the screw preload vanishes, the implant–abutment connection is provided by the tapered interference fit (TIF) alone. A close inspection of this figure shows that the condition where the change from TIS-type to TIF-type connection mechanism occurs at higher taper angles as the coefficient of friction increases. Therefore, it is concluded that in order to keep the screw preloaded, relatively high friction coefficient is necessary for large taper angles. This figure also suggests that, for the friction coefficient values considered here, the implant–abutment connection mechanism has switched from TIS to TIF for both Ankylos-like and ITI-like geometries, which have taper angles of 5.5° and 8°, respectively. However, this should have no adverse effects, because the tapered section of these abutments provides most of the resistance to loosening torque, as it will be shown later in the paper.

3.2. Effects of system parameters

The tightening and loosening torque formulas developed here provide a relatively simple way of assessing the effects of the geometric and material properties. For example, the magnitudes of the tightening torque T_T and loosening torque T_L, found in Eqs. (6) and (11),

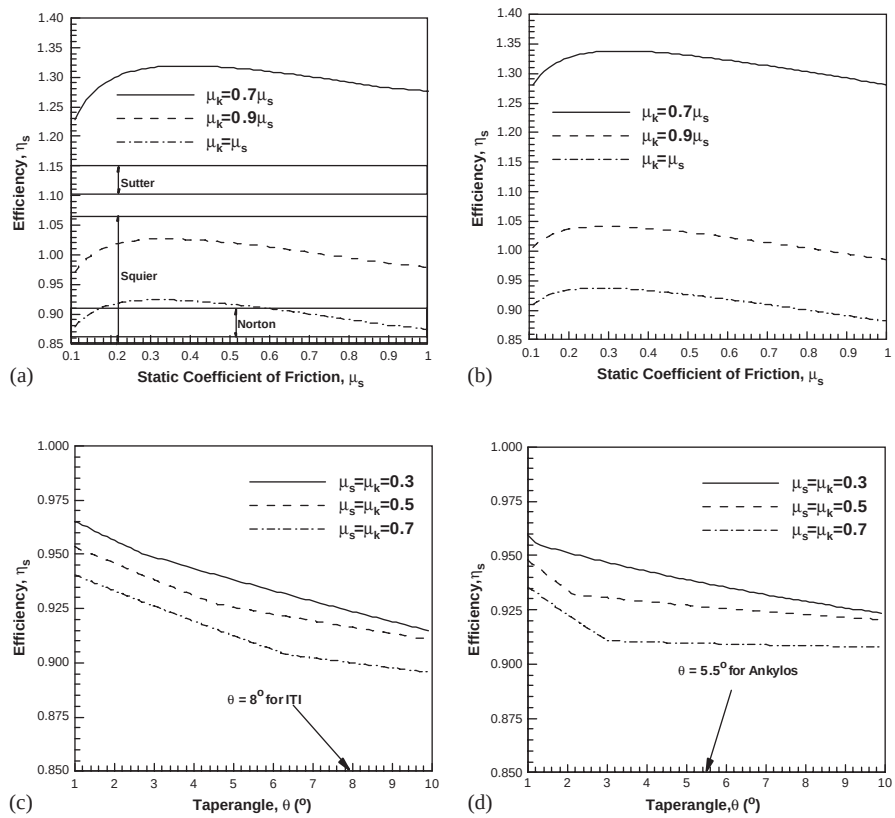

Fig. 6. The efficiency of the attachment with respect to different parameters. Taper angle θ, friction coefficient μ are the significant parameters affecting the efficiency of the attachment. Other parameters are given in Table 1. (a) ITI-like; (b) Ankylos-like; (c)ITI-like; (d) Ankylos-like.

depend on the parameters Δz and E, linearly; on the parameters b_2, r_{ab} parabolically; on the parameter L_c in a cubic manner; on the parameters θ and λ trigonometrically; and on the parameters μ_k, μ_s in a non-linear manner. The details of these functional dependencies for the ITI-like and Ankylos-like systems are given next, in Fig. 7. Unless otherwise specified the kinetic friction coefficient μ_k is taken to be equal to the static friction coefficient μ_s, in this figure.

Figs. 7a and b show the effect of taper angle θ on the tightening torque T_T and the loosening torque T_L for $\mu_k = \mu_s = 0.3$, 0.5 and 0.7, for the ITI-like and Ankylos-like systems, respectively. These figures indicate that the tightening torque is always greater than the loosening torque, for both systems, when the kinetic and static friction coefficients are identical. The difference between the tightening and loosening torque values increases for larger taper angles and at higher friction coefficient values. Note that the tightening torque values reported in this figure are conservative values, as the kinetic friction coefficient is taken to be the same as the static friction coefficient. However, the figure can be used as a guide in the design of the new TIS-type abutments. More detail on the T_T values can be easily obtained by using Eq. (11) for the case when kinetic friction coefficient is different than the static one.

Fig. 7c shows the effect of the contact length L_c of the tapered section of the abutment on the tightening and loosening torque values at different friction levels, for ITI- and Ankylos-like systems, respectively. In the contact length range, $0 < L_c < 5$ mm, considered in these figures, the tightening and loosening torque values increase with contact length, as expected. In this range, the rate of increase of T_T and T_L with L_c is nearly constant for the Ankylos-like system, whereas it decreases for the ITI-like system. This figure also demonstrates how the contact length L_c can be utilized as a design parameter, when the actual friction coefficient can be difficult to measure or subject to change with the short and long-term exposure to environmental conditions. For example, when the ITI-like system is considered the tightening torque value of $T_T = 400$ N mm can be obtained with $L_c = 0.35$ mm when $\mu_s = 0.7$; however, if the friction coefficient is lower, such as, $\mu_s = 0.3$ then a longer contact length of $L_c = 0.85$ mm could be used.

Fig. 7d shows the variation of the tightening and loosening torque values with the outer radius b_2 of the implant for both systems. This figure shows that higher torque values are required to tighten an implant, which has a larger outer radius. The loosening torque follows the same trend, however its value is predicted to be

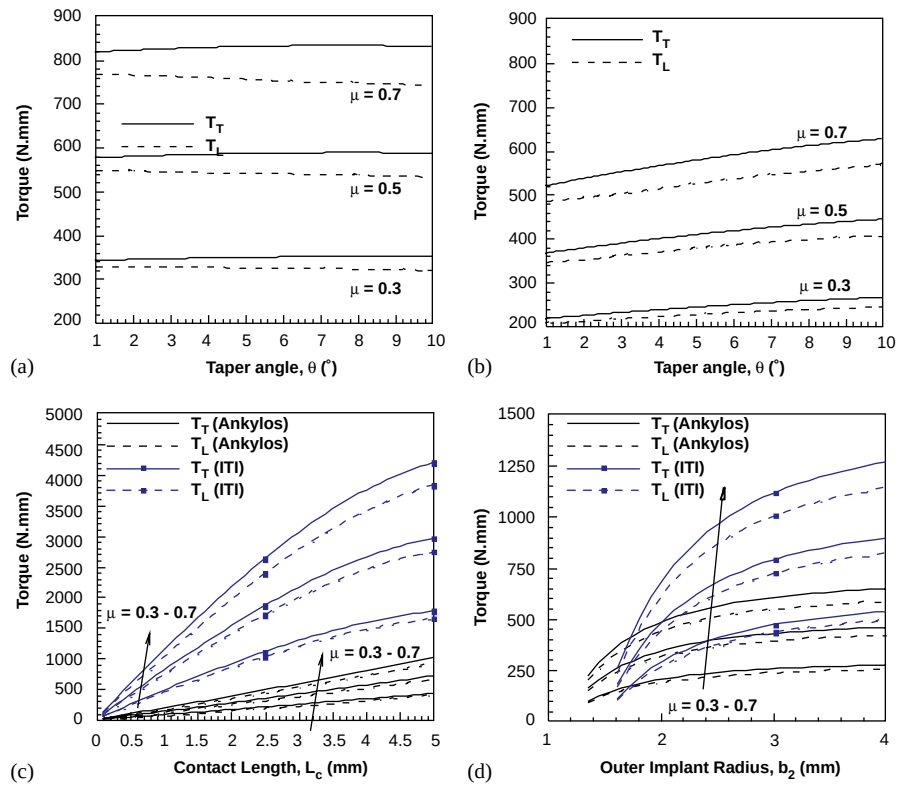

Fig. 7. The effect of taper angle θ (a, b); the contact length L_c (c); the outer radius of the implant b_2 (d) on loosening T_L and tightening T_T torques, for both ITI-like and Ankylos-like geometries. Note that friction coefficient $\mu_s = \mu_k = \mu$ for both systems. Other parameters are given in Table 1.

lower than the tightening torque when the kinetic and static friction coefficients are equal. Bozkaya and Müftü (2003) have shown that, in the tapered section, the contact pressure between the implant and the abutment increases with increasing implant radius. Thus larger normal and frictional forces develop in the interface, resulting in increased torque values.

A relation between the tightening torque and the loosening torque can be obtained from Eqs. (6) and (11), by noting that Δz is common in both relations. This shows that loosening torque is linearly proportional to the tightening torque as shown in Fig. 8. This finding is in agreement with the experimental data by Norton (1999) showing a linear relation between tightening and loosening torque. The slope of the curves, which is equal to the efficiency, is slightly different, which may stem from the difference in kinetic and static friction values. Note that this figure was obtained by using $\mu_k = \mu_s = 0.3$.

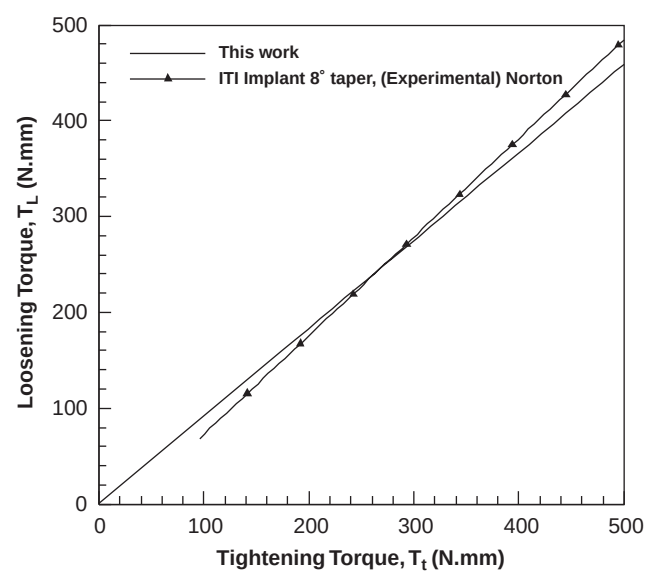

Fig. 8. The relation between the tightening torque T_T and the loosening torque T_L as predicted by this work and as measured by Norton (1999) for the ITI implant. Calculations were performed by using $\mu_k = \mu_s = 0.3$. Other parameters are given in Table 1.

3.3. Screw preload vs. torque

The screw preload as a function of relevant torque values can be obtained from Eqs. (6) and (11). Various preload conditions, for the ITI-like system, have been described in Fig. 9; the preload F_T^r during tightening, the preload during F_L^r loosening, and the preload F^r during functional loading are plotted as a function of torque for $\mu = 0.3$ and 0.5, in Fig. 9. This figure shows that, in general, the screw preload is linearly proportional to the applied torque. For a given torque value, the highest

preload occurs during tightening; after the release of the tightening torque, the screw is subjected to preload F^r. This is the "seated" preload of the screw. The preload becomes even lower during loosening.

Friction has an interesting effect on the preload; for a given torque value, the preload F^r reduces as the friction coefficient is increased. For example at 350 N mm the preload moves from 100 to 60 N, as the friction coefficient is increased from 0.3 to 0.5. Note that Merz et al. (2000) predicted 53 N of preload, by modeling a 12 mm long, 8° taper, TIS-type ITI implant with non-linear finite element analysis (Merz et al., 2000). The preload value of 60 N, predicted by the analytical method introduced here, is remarkably close to their value considering the assumptions made in this paper.

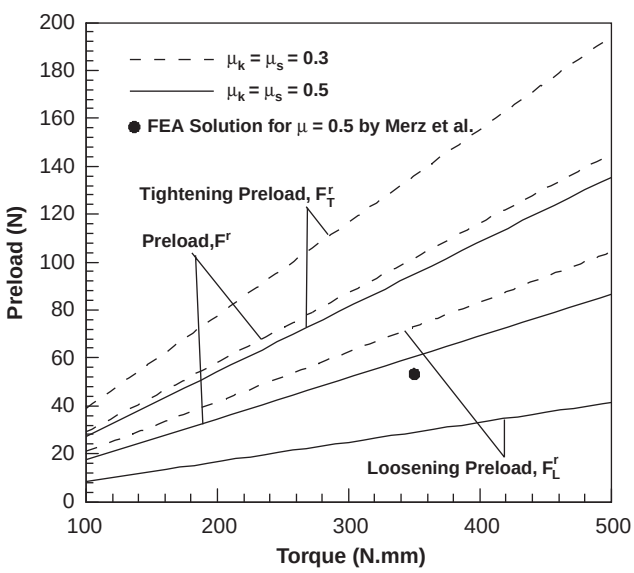

Fig. 9. Screw preload as a function of external torque for two different friction coefficients, for the ITI-like geometry. The indicated data point has been taken from Merz et al. (2000). Other parameters are given in Table 1.

3.4. Distribution of torque

The tapered surface of the TIS-type abutment provides a great deal of frictional resistance as compared to the frictional resistance on the screw threads. This is evidenced by the plots given in Fig. 10, where the percentage of the total tightening torque carried by the tapered section as a function of friction coefficient and taper angle θ are shown. This figure represents results for the ITI-like system.

In Fig. 10a, it is seen that, the tapered area resists 87–92% of the total torque during tightening, when the static friction coefficient μ_s is in the range 0.1–0.9. The kinetic friction μ_k coefficient has a relatively small effect on this percentage. The effect of the taper angle θ on the T_{taper}/T_{total} ratio during tightening is shown in Fig. 10b. This figure shows that in a TIS-type abutment with a smaller taper angle more of the total torque is carried by the tapered section, in contrast to larger taper angle. The range of T_{taper}/T_{total} ratio is between 88 and 96% depending on the value of static friction coefficient μ_s.

During loosening, the friction force in the screw threads act in a direction to reduce the screw preload as evidenced by Eq. (8). Thus, by varying the static friction coefficient μ_s or the taper angle θ it is possible to relieve the preload. When this happens all of the torque in the TIS-type abutment is carried by the tapered section, and the T_{taper}/T_{total} becomes one. The conditions which cause this are identified in Figs. 10a and b. In particular, Fig. 10a shows that friction coefficient values less than 0.15 would cause the loss of preload during loosening for an 8° taper. The effect of taper angle θ on the loss of preload depends on the value of the static friction coefficient μ_s as shown in Fig. 10b; increasing friction coefficient values allow use of larger taper angles before screw preload is lost during loosening. Also low static coefficient of friction in the screw threads μ_s may cause the screw torque to be negative, contributing to the loosening of the attachment. This happens when the

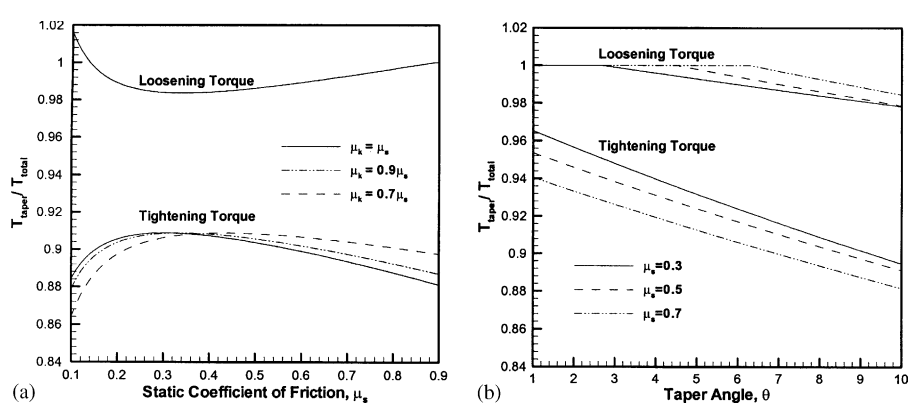

Fig. 10. The percentage of the total tightening torque carried by the tapered section as a function of (a) friction coefficient and (b) taper angle for the ITI-like geometry. Other parameters are given in Table 1.

static friction coefficient μ_s is smaller than 0.15 causing the T_{taper}/T_{total} to be larger than one.

4. Discussion

The general range of efficiency, predicted to be 0.85–1.37, for the range of parameters considered in this paper, match closely the experimental results (Squier et al., 2002; Norton 1999; Sutter et al., 1993). The only condition that causes the efficiency to be greater than 1.0 is encountered when the kinetic coefficient of friction is taken 10% smaller than the static coefficient of friction. The efficiency becomes as low as 0.85 for very low values of the coefficient of friction, such as 0.1. The efficiency also depends on the taper angle; an increase in taper angle from 1° to 10° results in a decrease in the efficiency, from 0.97 to 0.9, depending on the value of the friction coefficient.

Other causes for further losses known as 'embedment relaxation' which cause 2–10% reduction in the preload have been reported (Geng et al., 2001). Issues related to manufacturing tolerance, surface roughness, and creep of surface asperities are not captured by the analytical method presented here.

The apparent contact area, represented by the contact length L_c, affects the magnitudes of the tightening and loosening torques. However, L_c has a negligible effect on the efficiency of the two systems considered in this study. This indicates that the systems should be designed based on the tolerable torque levels for tightening and loosening; but, not on efficiency alone. A large value of loosening torque may be safer to prevent abutment loosening during functional loading of single tooth replacements, however, it requires a large tightening torque, as expected and as demonstrated here and by Norton (1999).

When all of the parameters that affect the tightening and loosening torque values, as given by Eqs. (6) and (11), are considered, it is seen that the taper angle θ, contact length L_c and outer radius of the implant b_2 have the strongest influence. It has been shown here that, among these three parameters, the contact length is the most practical parameter to adjust and has the strongest effect on increasing the loosening torque value.

The behavior of the TIS-type of abutment attachment method is governed by the tapered section of the abutment, as a large fraction of the loosening and tightening torque values are used to overcome the friction in the tapered section. The analytical method demonstrated that over 86% of the tightening torque, and over 98% of the loosening torque are balanced by the frictional resistance in the tapered section.

This study clearly shows that the value of the friction coefficient strongly affects tightening and loosening torque values. The friction coefficient is a property whose complexity is often underestimated. The friction coefficient depends on many factors including mechanical properties and the roughness of the contact interface, exposure to interfacial contaminants (Williams, 2000) and in some cases the normal load (Adams et al., 2003). In particular, the effects of contaminants are difficult to assess without extensive experiments. Therefore, a margin should be built into the design of the TIS-type abutments. Formulas developed in this work would provide guidance to this end.

Acknowledgements

The authors would like to thank Mr. Fred Weekley (United Titanium Inc., Wooster, OH, USA) for his valuable discussion related to this paper and acknowledge partial support of Bicon Implants (Bicon Inc., Boston, MA, USA).

References

Adams, G.G., Müftü, S., Mohd Azar, N., 2003. A scale-dependent model for multi-asperity model for contact and friction. Journal of Tribology 125, 700–708.

Andersson, B., Odman, P., Lindvall, A.M., Lithner, B., 1995. Single-tooth restorations supported by osseointegrated implants: results and experiences from a prospective study after 2 to 3 years. International Journal of Oral Maxillofacial Implants 10 (6), 702–711.

Anonymous, 2001. US markets for dental implants 2001: executive summary. Implant dentistry, 10(4), 234–237.

Anonymous, 2003. Ankylos Standard Abutment System. Friadent Product Catalogue, Friadent GmbH, P.O. Box 71 01 11, D-68221, Mannheim, Germany.

Aryatawong, K., Kamolpan, N., June 28–July 1, 1998. Antirotational effect of conical abutment/implant interface for single-tooth replacement. Proceedings of the 15th International Conference on Oral Biology, Baveno, Italy.

Becker, W., Becker, B.E., 1995. Replacement of maxillary and mandibular molars with single endosseous implant restorations: A retrospective study. Journal of Prosthetic Dentistry 74, 51–55.

Behneke, A., Behneke, N., d'Hoedt, B., 2000. The longitudinal clinical effectiveness of ITI solid-screw implants in partially edentulous patients: a 5-year follow-up report. International Journal of Oral Maxillofacial Implants 15, 633–645.

Bianco, G., Di Raimondo, R., Luongo, G., Paoleschi, C., Piccoli, P., Piccoli, C., Rangert, B., 2000. Osseointegrated implant for single-tooth replacement: a retrospective multicenter study on routine use in private practice. Clinical Implant Dentistry Related Research 2 (3), 152–158.

Bozkaya, D., Müftü, S., 2003. Mechanics of the tapered interference fit in dental implants. Journal of Biomechanics 36 (11), 1649–1658.

Bozkaya, D., Müftü, S., 2004. Efficiency considerations for the purely tapered interference fit (TIF) abutments used in dental implants. Journal of Biomechanical Engineering, accepted for publication.

Geng, J., Tan, K., Liu, G., 2001. Application of finite element analysis in implant dentistry: a review of the literature. Journal of Prosthetic Dentistry 85, 585–598.

Haas, R., Mensdorff-Pouilly, N., Mailath, G., Watzek, G., 1995. Branemark single tooth implants: a preliminary report of 76 implants. Journal of Prosthetic Dentistry 73 (3), 274–279.

Haas, R., Polak, C., Furhauser, R., Mailath-Pokorny, G., Dortbudak, O., Watzek, G., 2002. A long-term follow-up of 76 Branemark single-tooth implants. Clinical Oral Implants Research 13 (1), 38–43.

Jansen, V.K., Richter, E.J., 1997. Microbial leakage and marginal fit of the implant-abutment interface. International Journal of Oral Maxillofacial Implants 12, 527–540.

Jemt, T., Laney, W.R., Harris, D., Henry, P.J., Krogh Jr, P.H.J., Polizzi, G., et al., 1991. Osseointegrated implants for single tooth replacement: a 1-year report forma multicenter prospective study. International Journal of Oral Maxillofacial Implants 6, 29–36.

Lang, L.A., Kang, B., Wang, R.-F., Lang, B.R., 2003. Finite element analysis to determine implant preload. Journal of Prosthetic Dentistry 90, 539–546.

Levine, R.A., Clem, D.S., Wilson Jr., T.G., Higginbottom, F., Solnit, G., 1997. Multicenter retrospective analysis of the ITI implant system used for single-tooth replacements: Preliminary results at 6 or more months of loading. International Journal of Oral Maxillofacial Implants 12, 237–242.

Levine, R.A., Clem, D.S., Wilson Jr., T.G., Higginbottom, F., Saunders, S.L., 1999. A multicenter retrospective analysis of the ITI implant system used for single-tooth replacements: results of loading for 2 or more years. International Journal of Oral Maxillofacial Implants 14, 516–520.

Merz, B.R., Hunenbart, S., Belser, U.C., 2000. Mechanics of the implant–abutment connection: an 8-degree taper compared to a butt joint connection. International Journal of Oral Maxillofac Implants 15, 519–526.

Misch, C.E., 1999. Principles for screw-retained prosthesis. In: Misch, C.E. (Ed.), Contemporary Implant Dentistry. Mosby, St. Louis, Missouri, pp. 575–598.

Norton, M.R., 1999. Assessment of cold welding of the internal conical interface of two commercially available implant systems. Journal of Prosthetic Dentistry 81, 159–166.

Norton, M.R., 2000. In vitro evaluation of the strength of the conical implant-to-abutment joint in two commercially available implant systems. Journal of Prosthetic Dentistry 83, 567–571.

O'Callaghan, J., Goddard, T., Birichi, R., Jagodnik, J., Westbrook, S., 2002. Abutment hammering tool for dental implants. IMECE-2002 Proceedings, Vol. 2, American Society of Mechanical Engineers, November 11–16, 2002, Paper No. DE-25112.

Romanos, G.E., Nentwig, G.H., 2000. Single molar replacement with a progressive thread design implant system: a retrospective clinical report. International Journal of Oral Maxillofacial Implants 15, 831–836.

Scacchi, M., Merz, B.R., Schär, A.R., 2000. The development of the ITI dental implant system. Clinical Oral Implants Research 11 (Suppl.), 22–32.

Schwarz, M.S., 2000. Mechanical complications of dental implants. Clinical Oral Implants Research 2000 11 (Suppl.), 156–158.

Scheller, H., Urgell, J.P., Kultje, C., Klineberg, I., Goldberg, P.V., Stevenson-Moore, P., Alonso, J.M., et al., 1998. A 5-year multicenter study on implant-supported single crown restorations. International Journal of Oral Maxillofacial Implants 13 (2), 212–218.

Shigley, J.E., Mischke, C.R., 1989. Mechanical Engineering Design, 5th edition, McGraw Hill, Boston, pp. 450–457.

Squier, R.S., Psoter, W.J., Taylor, T.D., 2002. Removal torques of conical, tapered implant abutments: The effects of anodization and reduction of surface area. International Journal of Oral Maxillofac Implants 17, 24–27.

Sutter, F., Weber, H.P., Sorensen, J., Belser, U., 1993. The new restorative concept of the ITI dental implant system: design and engineering. International Journal of Periodontics Restorative Dentistry 13, 409–431.

Wannfors, K., Smedberg, J.-I., 1999. A prospective evaluation of different single tooth restoration designs on osseointegrated implants. A 3-year follow-up of Branemark implants. Clinical Oral Implant Research 10, 453–458.

Williams, J.A., 2000. Engineering Tribology. Oxford University Press, Oxford, UK.